Journal of Theoretical Biology 317 (2013) 20–29

Contents lists available at SciVerse ScienceDirect

Journal of Theoretical Biology

journal homepage: www.elsevier.com/locate/yjtbi

Mathematical model of colitis-associated colon cancer

Wing-Cheong Lo [a,*], Edward W. Martin Jr. [b], Charles L. Hitchcock [c], Avner Friedman [a,d]

[a] Mathematical Biosciences Institute, The Ohio State University, Columbus, OH 43210, USA
[b] Division of Surgical Oncology, Department of Surgery, Arthur G James Cancer Hospital and Richard J Solove Research Institute and Comprehensive Cancer Center, The Ohio State University, Columbus, OH 43210, USA
[c] Department of Pathology, The Ohio State University, Columbus, OH 43210, USA
[d] Department of Mathematics, The Ohio State University, Columbus, OH 43210, USA

HIGHLIGHTS

- First ever mathematical model of colitis-associated colon cancer.
- Multiscale approach connecting genes mutations to epithelium proliferation.
- *TP53* mutation and inflammed colonic mucosa contribute to cancer early development.
- *TP53* mutations play a primary role, followed by *APC* mutation.

ARTICLE INFO

Article history:
Received 15 May 2012
Received in revised form
28 August 2012
Accepted 18 September 2012
Available online 28 September 2012

Keywords:
Colorectal cancer
Mucin
APC
TP53
Mathematical model

ABSTRACT

As a result of chronic inflammation of their colon, patients with ulcerative colitis or Crohn's disease are at risk of developing colon cancer. In this paper, we consider the progression of colitis-associated colon cancer. Unlike normal colon mucosa, the inflammed colon mucosa undergoes genetic mutations, affecting, in particular, tumor suppressors *TP53* and adenomatous polyposis coli (*APC*) gene. We develop a mathematical model that involves these genes, under chronic inflammation, as well as NF-κB, β-catenin, MUC1 and MUC2. The model demonstrates that increased level of cells with *TP53* mutations results in abnormal growth and proliferation of the epithelium; further increase in the epithelium proliferation results from additional *APC* mutations. The model may serve as a conceptual framework for further data-based study of the early stage of colon cancer.

1. Introduction

Colorectal cancer (CRC) is the second leading cause of cancer-related deaths worldwide (Ferlay et al., 2010). Several gene mutations have been identified to have occurred in the early stages of the disease, including *APC*, *TP53*, *K-RAS* and *SMAD* (Rowan et al., 2000). In this paper, we focus on colon cancer; more specifically, on colitis-associated colon cancer. Patients with ulcerative colitis or Crohn's disease are at risk of developing CRC as a result of chronic inflammation of their colon. Unlike cells of the normal colonic mucosa, cells of the inflammed colonic mucosa undergo genetic alteration, such as *TP53* mutation, prior to dysplasia or cancer (Ullman and Itzkowitz, 2011).

Mutations inactivating the *APC* gene are found in 80% of all human colon cancer (Kwong and Dove, 2009). While *APC* inactivation is believed to occur early in sporadic colon cancer (i.e., before early adenoma), the inactivation of *TP53* occurs much earlier in colitis-associated colon cancer (Ullman and Itzkowitz, 2011). Loss of heterozygosity at p53 in colitis-associated colon cancer correlates with malignant progression, and was detected in 63% high grade dysplasia prior to *APC* inactivation (Ullman and Itzkowitz, 2011). As reported in Ullman and Itzkowitz (2011), *TP53* mutations were found in inflammed mucosa of more than 50% of patients who did not have cancer.

The colonic mucosa forms a barrier against bacterial infection of the colonic epithelium. It consists of several mucins, primarily mucin 2 (MUC2) which is released from the epical membrane, and mucin 1 (MUC1) which is a transmembrane mucin that lines the surface of epithelial cells. MUC1 and MUC2, mainly MUC2, suppress inflammation in the intestinal tract and inhibit the development of colon cancer by forming a protective barrier (Ueno et al., 2008; Velcich et al., 2002). MUC2 expression is upregulated by p53 protein (Ookawa et al., 2002). When *TP53* is mutated, MUC2 is downregulated resulting in a process that leads

* Corresponding author. Tel.: +1 9493949463.
E-mail address: lo.75@mbi.osu.edu (W.-C. Lo).

0022-5193/$ - see front matter © 2012 Elsevier Ltd. All rights reserved.
http://dx.doi.org/10.1016/j.jtbi.2012.09.025

to colon cancer. Indeed, chronic inflammation sets in, activating NF-κB which promotes cell growth and proliferation (Karin and Greten, 2005; Kojima et al., 2004). NF-κB also upregulates MUC1 and this further induces proliferation by stabilizing β-catenin (Huang et al., 2003; Kufe, 2009; Yamamoto et al., 1997). *APC* mutations are present frequently in mucin-depleted foci (MDF) through an inflammation-related pathway (Femia et al., 2007; Yang et al., 2008). *APC* mutation promotes inappropriate proliferation by upregulating intracellular inventory of active β-catenin available to cadherins (Bienz and Hamada, 2004).

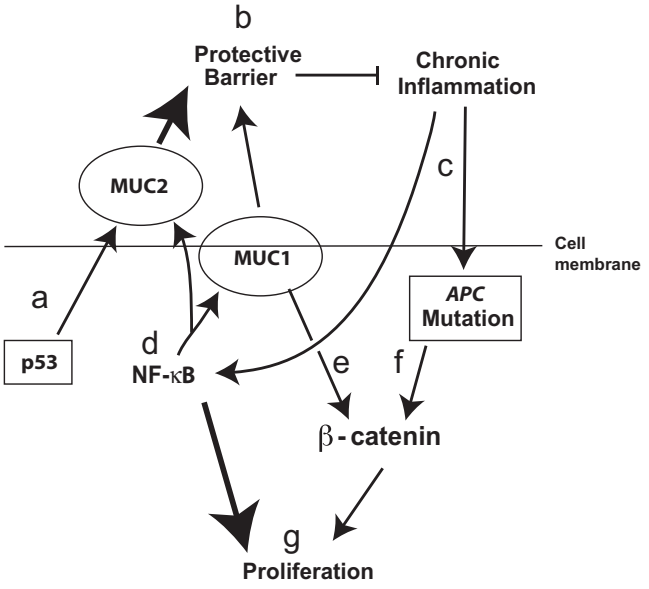

Fig. 1. Schematic diagram showing how MUC1 and MUC2 are involved in colitis-associated colon cancer in a cell. MUC1 is a transmembrane mucin lining the cellular surface and MUC2 is a secreted mucin released from apical membrane. (a) MUC2 expression is upregulated by p53 protein (Ookawa et al., 2002). (b) MUC1 and MUC2, mainly MUC2, suppress inflammation in the intestinal tract and inhibit the development of colon cancer by forming a protective barrier (Ueno et al., 2008; Velcich et al., 2002). (c) Adenomatous polyposis coli (*APC*) mutations are present frequently in mucin-depleted foci (MDF) through an inflammation-related pathway (Femia et al., 2007; Yang et al., 2008). (d) The production of inflammatory cytokines by immune effector cells activates nuclear factor-κB (NF-κB), which promotes cell growth and upregulates mucin expression to enhance the protective barrier (Karin and Greten, 2005; Iwashita et al., 2003; Li et al., 1998). (e) Overexpression of MUC1 in chronic inflammation induces proliferation and tumor progression through stabilizing β-catenin (Huang et al., 2003; Kufe, 2009; Yamamoto et al., 1997). (f) *APC* mutation promotes inappropriate proliferation by upregulating intracellular inventory of active β-catenin available to cadherins (Bienz and Hamada, 2004). (g) Proliferation of tumor in colon crypt is upregulated by active NF-κB (Karin and Greten, 2005; Kojima et al., 2004) and active β-catenin (Aust et al., 2001; Calvisi et al., 2004; Chen et al., 2008) under the simplifying assumption that the proliferation is mainly contributed by NF-κB.

In this paper, we develop a mathematical model of colitis-associated colon cancer. The model involves MUC1, MUC2, *TP53*, *APC*, NF-κB and β-catenin. Chronic inflammation is an important component of the model, although we model it just in a generic fashion by lumping together all its components. The goal of our mathematical model is to demonstrate in qualitative terms how mutations (inactivation) in *TP53*, possibly also followed by mutation in *APC*, result in tumor growth. The biological background of the model is shown schematically in Fig. 1, with more details in the section on "Mathematical Model".

van Leeuwen et al. (2006) reviewed the theoretical models of crypt dynamics and CRC, up to the year 2005, including hereditary syndromes, molecular dynamics and genetic instability, and CRC treatment; they also presented (see also van Leeuwen et al., 2007) a stochastic model of *APC* inactivation. Johnston et al. (2007) developed a mathematical model of population dynamics in colonic crypt and in CRC. A population dynamics approach which involves CRC progression through $APC \rightarrow K-RAS \rightarrow TP53$ mutations was presented by Michor et al. (2005) and Delitala and Lorenzi (2011).

To the authors' knowledge, the present paper is the first mathematical model of colitis-associated colon cancer. Although the genetic pathway leading to this carcinoma is quite complex, we believe that our simplified model is a useful first step to gain qualitative understanding of the early evolution of the disease.

2. Mathematical model

The mathematical model of colitis-associated CRC is based on the schematics of biological network shown in Fig. 1. The geometry of the colonic crypt is shown in Fig. 2A. In the mathematical model, we simplify this geometry, as shown in Fig. 2B, by resorting to a one-dimensional geometry where the apical membrane of the epithelium is a flat surface $x=0$, above which lies the mucus layer $\{0 < x < x_{top}\}$, and below which is the epithelium tissue $\{-x_m < x < 0\}$.

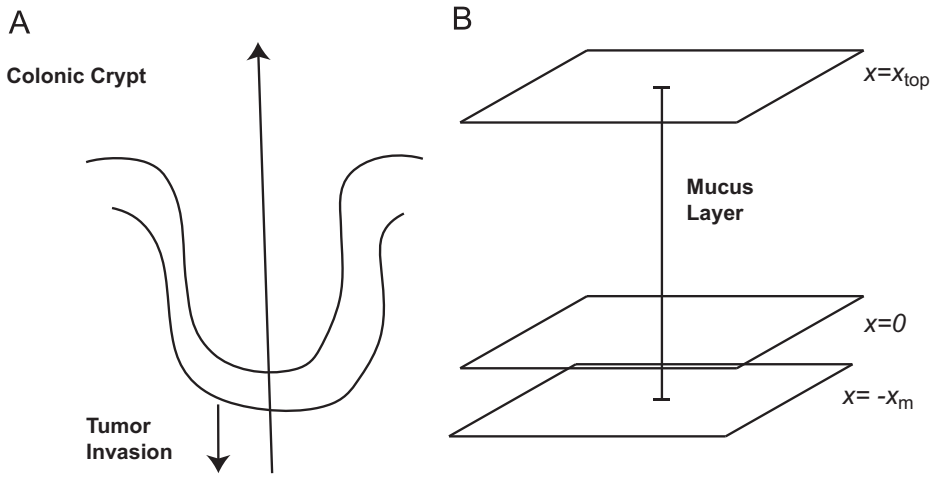

Fig. 2. The geometry of the model. (A) The colonic crypt and basement membrane. (B) A simplified one-dimensional model. The line $x=0$ is the apical surface of the colonic crypt. The region $\{0 < x < x_{top}\}$ represents the colonic crypt occupied by MUC2. The region $\{-x_m < x < 0\}$ represents the colonic epithelium; in this region, there are goblet cells, enterocytes, neuroendocrine cells, and colonic stems cells (Humphries and Wright, 2008). For simplification, we lump all the cells together and, furthermore, assume that tumor invasion goes only downwards.

2.1. Notations

We introduce the following notation:

p	level, or prevalence, of cells with *TP53* mutation
$M_1(t)$	concentration of MUC1 in tumor tissue (g/cm^3)
$M_2(x,t)$	concentration of MUC2 (g/cm^3) in the region $\{0<x<x_{top}\}$ above the apical membrane outside of the cells
$I(t)$	level of inflammatory response in tumor tissue
$N(t)$	concentration of active NF-κB (g/cm^3) in tumor tissue
$B(t)$	concentration of active β-catenin in tumor tissue (g/cm^3)
$x_m(t)$	thickness of tumor cells tissue (cm)

The variables satisfy a system of ordinary differential equations and the parameters of the system are given in Tables B1 and B2.

2.2. Mucins

MUC1 is a transmembrane mucin which lines the apical surface of epithelial cells and provides a protective barrier that can be upregulated to suppress inflammation caused by pathogenic bacteria (Linden et al., 2008; McGuckin et al., 2011). The expression of MUC1 is induced by inflammatory cytokines such as TNFα, IFNγ and IL-6 through NF-κB pathway (Saeland et al., 2012). The dynamic of the concentration of MUC1 is modeled as

$$\frac{dM_1}{dt}=\lambda_{11}+\underbrace{\alpha\frac{N}{N+K_1}}_{\text{production by NF-}\kappa\text{B}}-\underbrace{\lambda_{12}M_1}_{\text{degradation}}, \tag{1}$$

where λ_{11} is the basel production rate of MUC1 and λ_{12} is the degradation rate of MUC1.

MUC2 is a major secreted mucin which is released from the apical membrane to the region above $x=0$ and below some level $x=x_{top}$. It is a protective gel that suppresses the inflammatory response (Velcich et al., 2002; Linden et al., 2008; Allen et al., 1998; Byrd and Bresalier, 2004). MUC2 is diffusive above the apical surface with a diffusion coefficient D_M. We assume that the concentration of MUC2 satisfies a diffusion equation in the region $\{0<x<x_{top}\}$,

$$\frac{\partial M_2}{\partial t}=\underbrace{D_M\frac{\partial^2 M_2}{\partial x^2}}_{\text{diffusion}}-\underbrace{\lambda_{22}M_2}_{\text{degradation}}, \tag{2}$$

where λ_{22} is the degradation coefficient of MUC2.

MUC2 production is upregulated by NF-κB and *TP53* so that the combined production rate is proportional to $\lambda_{21}(p)+\beta N/(N+K_2)$ where $\lambda_{21}(p)$ depends on *TP53* in the following way: as the number of cells that developed *TP53* mutation is increased, the parameter $\lambda_{21}(p)$ is correspondingly decreased. We assume that this production rate results in a flux at the apical surface of the colon,

$$\left.\frac{\partial M_2}{\partial x}\right|_{x=0}=-\left(\lambda_{21}(p)+\beta\frac{N}{N+K_2}\right).$$

We also assume that MUC2 does not diffuse beyond the edge $x=x_{top}$, so that

$$\left.\frac{\partial M_2}{\partial x}\right|_{x=x_{top}}=0.$$

By integrating both sides of Eq. (2) from $x=0$ to $x=x_{top}$ and using the flux conditions, we obtain

$$\frac{d\int_0^{x_{top}}M_2dx}{dt}=D_M\left(\lambda_{21}(p)+\beta\frac{N}{N+K_2}\right)-\lambda_{22}\int_0^{x_{top}}M_2\,dx.$$

We define the total amount of M_2 in the region $\{x>0\}$ as $\hat{M}_2=\int_0^{x_{top}}M_2\,dx$. Then the dynamics of $\hat{M}_2$ is given by

$$\frac{d\hat{M}_2}{dt}=\underbrace{D_M\left(\lambda_{21}(p)+\beta\frac{N}{N+K_2}\right)}_{\text{production by cells}}-\underbrace{\lambda_{22}\hat{M}_2}_{\text{degradation}}.$$

2.3. Chronic inflammation

Chronic inflammation is not always in response to bacterial infection. The etiology of chronic inflammation includes autoimmune disease, viral or fungal infections, and other toxins. However, in the case of inflammatory bowel disease (ulcerative colitis and Crohn's disease), the main cause and accelerator of chronic inflammation are the bacterial infection (Ullman and Itzkowitz, 2011; Aggarwal et al., 2006). When the mucosal layer is damaged, the opportunity of bacterial infection increases and the inflammatory response is upregulated. We assume that the level of inflammatory response per cell, I, increases when the concentrations of MUC1 and MUC2 decrease, and take it to be

$$I=(1-M_1/\mu_1-\hat{M}_2/\mu_2)^+, \tag{3}$$

where $s^+=s$ if $s>0$ and $s^+=0$ if $s\le 0$. The parameters μ_1 and μ_2 are the normalizing factors of M_1 and $\hat{M}_2$, respectively.

2.4. NF-κB *and* β-catenin

NF-κB is activated by inflammatory cytokines during colitis-associated inflammation,

$$\frac{dN}{dt}=\underbrace{\lambda_{31}\left(1+\gamma\frac{(I/K_N)}{(I/K_N)+1}\right)}_{\text{activation}}-\underbrace{\lambda_{32}N}_{\text{deactivation}}, \tag{4}$$

where λ_{31} is the basal growth rate, λ_{32} is thedeactivation rate andK_N is the normalizing factor of I.

MUC1 cytoplasmic tail interacts with β-catenin and blocks the phosphorylation-dependent degradation of β-catenin. Overexpression of MUC1 increases stabilization of β-catenin (Huang et al., 2003). *APC* inactivation by chronic inflammation also reduces the *APC*-mediated β-catenin destruction (Bienz and Hamada, 2004). For simplicity, we assume that the effect of *APC* mutation on the degradation of β-catenin is proportional to the level of inflammatory response. The equation of β-catenin can then be written as follows:

$$\frac{dB}{dt}=\underbrace{\lambda_{41}}_{\text{production}}\underbrace{-\lambda_{42}\left(1+\frac{v_1}{1+(M_1/K_{B1})}+\frac{v_2}{1+\eta_A(I/K_{B2})}\right)B}_{\text{degradation}}, \tag{5}$$

where λ_{41} is the basal production rate of β-catenin per cell, λ_{42} is the degradation coefficients of β-catenin in a natural turnover, and η_A is the parameter controlling the level of *APC* mutation($\eta_A=0$ if *APC* is not mutated). K_{B1} and K_{B2} are the normalizing factors of M_1 and I, respectively.

2.5. Tumor cell

The tumor tissue consists of the extracellular matrix and several types of cells, including endothelial cells, macrophages, lymphocytes, fibroblasts, smooth muscle cells and, of course, (epithelial) cancer cells. Since the cancer cells are proliferating abnormally, the tumor tissue grows, and the cancer cells move with the growing tissue at some velocity $V(x,t)$. We denote density of the cancer cells by $C(x,t)$. Then, by conservation of

mass,

$$\frac{\partial C}{\partial t}+\underbrace{\frac{\partial (VC)}{\partial x}}_{\text{migration}}=\underbrace{\lambda_C(B,N)C}_{\text{proliferation}}, \tag{6}$$

in $\{-x_m<x<0\}$, where λ_C is the proliferation rate of cancer cells. The proliferation rate depends on the concentration of active NF-κB (Karin and Greten, 2005; Kojima et al., 2004) and active β-catenin (Aust et al., 2001; Calvisi et al., 2004; Chen et al., 2008); we assume that NF-κB plays a somewhat larger role than β-catenin, andcancer cells do not proliferate if the sum of normalized B and N is less than a threshold K_C; accordingly we take

$$\lambda_C(B,N)=\lambda_{51}\frac{(0.8B/B_{ss}+N/N_{ss}-K_C)^+}{(0.8B/B_{ss}+N/N_{ss}-K_C)^++1}. \tag{7}$$

where N_{ss} and B_{ss} are the steady state concentrations of NF-κB and β-catenin, respectively, in healthy tissue.

We assume for simplicity that the cells density in the tissue $\{-x_m<x<0\}$ is a constant, C_0, so that Eq. (6) becomes

$$C_0\frac{\partial V}{\partial x}=\lambda_C(B,N)C_0. \tag{8}$$

Assuming also that the velocity at the top of the epithelium is zero, we get

$$-V(-x_m)=\lambda_C(B,N)x_m. \tag{9}$$

Hence the dynamic of $x=-x_m$ is governed by the following equation,

$$\frac{dx_m}{dt}=\lambda_C(B,N)x_m. \tag{10}$$

2.6. Governing equations

Combining all the above equations, we have

$$\frac{dM_1}{dt}=\lambda_{11}+\underbrace{\alpha\frac{N}{N+K_1}}_{\text{production by NF-}\kappa\text{B}}-\underbrace{\lambda_{12}M_1}_{\text{degradation}}, \tag{11}$$

$$\frac{d\hat{M}_2}{dt}=\underbrace{D_M\left(\lambda_{21}(p)+\beta\frac{N}{N+K_2}\right)}_{\text{production by cells}}-\underbrace{\lambda_{22}\hat{M}_2}_{\text{degradation}}, \tag{12}$$

$$\frac{dN}{dt}=\underbrace{\lambda_{31}\left(1+\gamma\frac{(I/K_N)}{(I/K_N)+1}\right)}_{\text{activation}}-\underbrace{\lambda_{32}N}_{\text{deactivation}}, \tag{13}$$

$$\frac{dB}{dt}=\underbrace{\lambda_{41}}_{\text{production}}\underbrace{-\lambda_{42}\left(1+\frac{v_1}{1+(M_1/K_{B1})}+\frac{v_2}{1+\eta_A(I/K_{B2})}\right)B}_{\text{degradation}}, \tag{14}$$

$$\frac{dx_m}{dt}=\lambda_C(B,N)x_m, \tag{15}$$

with

$$I=(1-M_1/\mu_1-\hat{M}_2/\mu_2)^+ \tag{16}$$

and

$$\lambda_C(B,N)=\lambda_{51}\frac{(0.8B/B_{ss}+N/N_{ss}-K_C)^+}{(0.8B/B_{ss}+N/N_{ss}-K_C)^++1}. \tag{17}$$

3. Simulations

The simulations described in this section were performed using the Matlab build-in solver ode23. The parameters used in the simulations were determined in Appendix A and are summarized in Tables B1 and B2.

Figs. 3–5 show how the thickness of the epithelium, x_m, increases in time under mutations of *TP53* and *APC*; time, along the horizontal axis, is measured in hours, and x_m, along the vertical axis, is measured in cm.

Mutation in *TP53* is represented by the parameter $\lambda_{21}(p)$:as more cells undergo *TP53* mutation, this parameter $\lambda_{21}(p)$ decreases, and the thickness $x_m=x_m(t)$ increases. Similarly, as more cells undergo *APC* mutation, the parameter η_A increases, and x_m still further increases.

In Fig. 3 we see, at different fixed values of η_A, a dramatic increase in x_m as $\lambda_{21}(p)$ decreases from 3.31 (low level of *TP53*

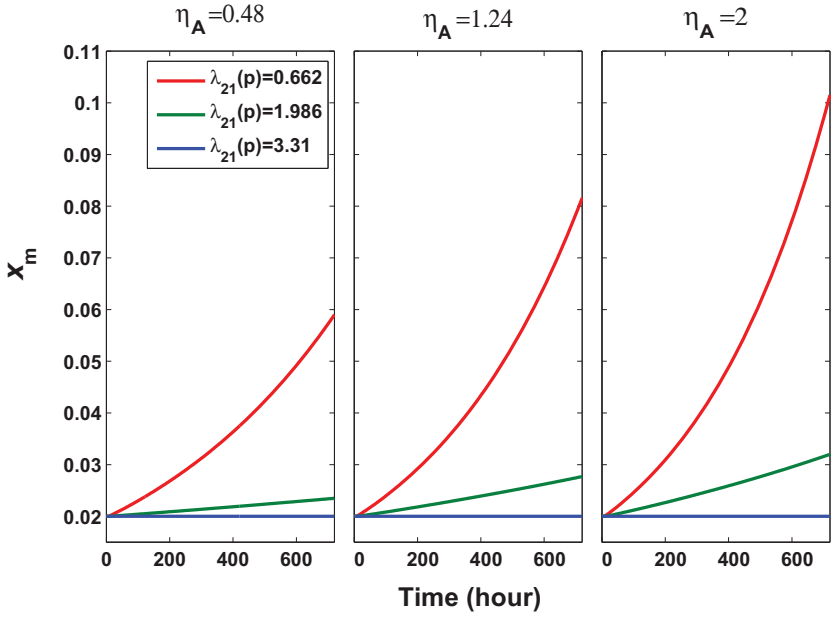

Fig. 3. Time evolution of tumor thickness for different levels of *TP53* mutation. When level of *TP53* mutation, p, increases, the production rate of MUC2, λ_{21}, decreases. In each subplot, η_A is fixed. The horizontal axis measures timein hours and the vertical axis measures the tumor thickness x_m in cm.

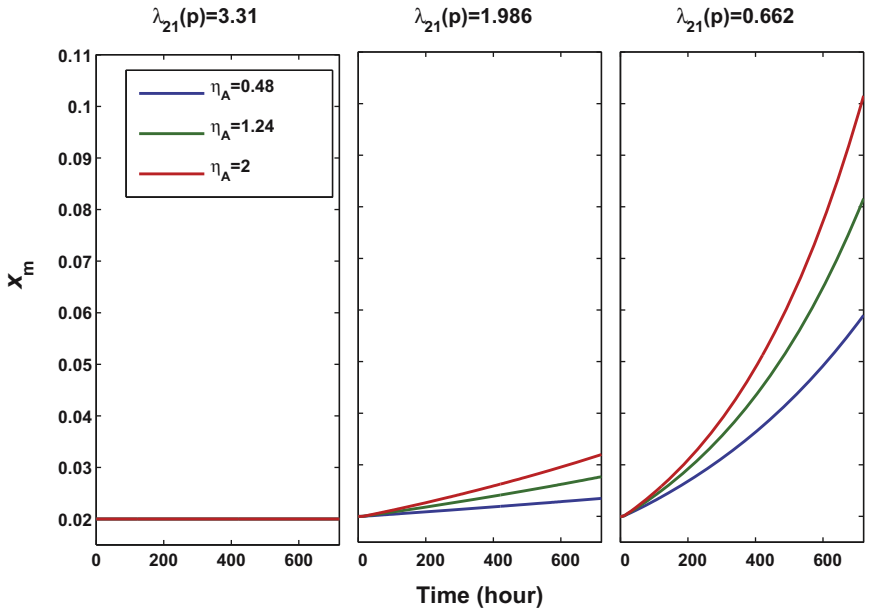

Fig. 4. Time evolution of tumor thickness for different levels of *APC* mutation. When level of *APC* mutation increases, η_A increases. In each subplot, η_A is fixed. The horizontal axis measures time in hours and the vertical axis measures the tumor thickness x_m in cm.

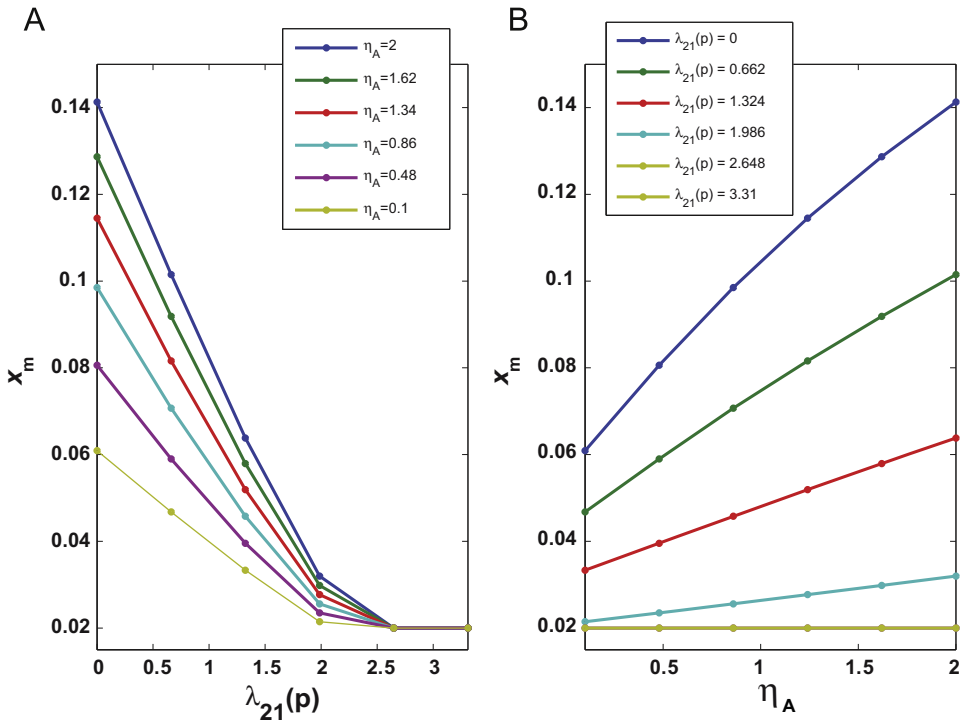

Fig. 5. Tumor thickness at time 720 h under mutations of *TP53* and *APC*. (A) Tumor thickness x_m after 720 h as a function of the parameter $\lambda_{21}(p)$ for different values of η_A. (B) Tumor thickness x_m after 720 h as a function of the parameter η_A for different values of $\lambda_{21}(p)$. The curves with $\lambda_{21}(p)=3.31$ and $\lambda_{21}(p)=2.648$ essentially coincide.

mutations among the epithelial cells) to 0.662 (high level of *TP53* mutations). Fig. 4 shows, at different fixed values of $\lambda_{21}(p)$, an increase in x_m as the parameter η_A is increased from 0.48 (low level of *APC* mutation among the epithelial cells) to 2 (high level of *APC* mutations). We note that the increase in x_m as a result of *APC* mutations is relatively mild compared with the increase resulting from *TP53* mutations. This is consistent with the fact that in colitis-associated colon cancer, the initial mutation of *TP53* plays a more major role than *APC* mutation.

In Fig. 5A, we plotted the thickness x_m after 720 h as a function of the parameter $\lambda_{21}(p)$ for different values of η_A; as $\lambda_{21}(p)$ decreases (more *TP53* mutations occurred among the cells), x_m increases. For larger values of η_A (more cells underwent also *APC* mutations), the level of x_m is increased, although the relative increase, as η_A increases, is rather mild.

On the other hand, Fig. 5B shows a much larger increase of x_m after 720 h as $\lambda_{21}(p)$ decreases from 3.31 (no *TP53* mutation) to 0 (high level of *TP53* mutations). The depth of the proliferating epithelium, x_m, is further increased with additional *APC* mutations, i.e., as η_A increases so does the x_m-graph. This increase, however, is very mild when the level of *TP53* mutation is small ($\lambda_{21}(p)=2.648$, 3.31) and it becomes more

pronounced when the level of *TP53* mutations is high ($\lambda_{21}(p) = 0, 0.662$).

The simulations in Figs. 3–5 show that *TP53* inactivation plays a major role in colitis-associated tumor growth, while *APC* inactivation plays only a secondary role, which is quite minor, unless the level of *TP53* mutations among the epithelial cells has become large enough. This lends support to the hypothesis that in colitis-associated colon cancer, *TP53* mutation plays more significant role than *APC* mutation, at least in the early stage of the disease.

4. Sensitivity analysis

Since the normalizing factors (i.e., K_2, K_N, K_{B1}, K_{B2}, μ_1, μ_2, B_{ss} and N_{ss}) in the model were only roughly estimated, we performed sensitivity analysis to determine the robustness of the simulation results and effect of the parameters on x_m. We used the method of Partial Rank Correlation Coefficient (PRCC) (Marino et al., 2008) for our sensitivity analysis. We ran 5000 simulations in which the parameters were varied according to Latin hypercube sampling scheme with the ranges shown in Table B3. In all the simulations, $\eta_A = 1$ and $\lambda_{21}(p) = 0.662\ \mathrm{g/cm^4}$. The results of the sensitivity analysis are summarized in Table B3. Fig. 6 shows the scatter plots of rank transformed x_m at 720 h versus the rank transformed parameters with significant correlation; the title of each subplot shows its PRCC value and statistical significance.

We see that the only statistically significant PRCC values are B_{ss}, N_{ss}, μ_1, μ_2, K_{B1}, K_{B2} and K_N; among them, the parameters B_{ss}, N_{ss} and μ_1 have PRCC values larger than 0.5 in magnitude. The parameters B_{ss} and N_{ss} are negatively correlated to x_m, which is indeed natural: when these normalizing factors increase, the velocity $\lambda_C(B,N)$ of x_m decreases. On the other hand, μ_1 and μ_2 are positively correlated to x_m: as they increase, the inflammation I increases and so does x_m. Note that μ_2 correlates more strongly to x_m than μ_1, indicating that MUC2 is more prominent than MUC1 in providing protective barrier against inflammation. Finally, according to Table B3 and Fig. 6, the other normalizing factors (K_1, K_2, K_N, K_{B1}, K_{B2}) as well as the other parameters do not affect x_m appreciably.

5. Conclusion and discussion

Colorectal cancer is one of the most common types of cancer around the world. A significant number of colon cancer cases are associated with chronic inflammation resulting from ulcerative colitis or Crohn's disease. This inflammation arises from the immune system response to bacterial infection, which occurs when the colonic mucosa undergoes genetic alterations. Such alterations can be traced to tumor suppressor gene *TP53* which regulates MUC2 production. Other mutations may also subsequently occur, such as *APC* inactivation. Although *APC* is involved in a number of signaling pathways, here we consider its effect just in terms of its response to inflammation, where it plays only a secondary role.

Our model includes *TP53*, NF-κB and β-catenin, MUC1 and MUC2, and the level of chronic inflammation. We measure the degree of tumor cells proliferation by the combined levels of NF-κB and β-catenin. The simulations illustrate how increased level of *TP53* mutation among colonic epithelial cells results in increased proliferation of the epithelium into the stroma. Mutations in *APC* in the context of colitis-associated colon cancer contributed only slightly to cells proliferation, as compared to *TP53* mutations.

Our model is multi-scale: it includes processes that occur within cells,and, at the same time, it treats cells proliferation at the tissue level, showing increase in the thickness of the epithelium as a result of *TP53* and *APC* mutations. The model is formulated by a system of differential equations. Most of the parameters have been determined from theliterature, directly or indirectly, but a few parameters, especially the "normalizing

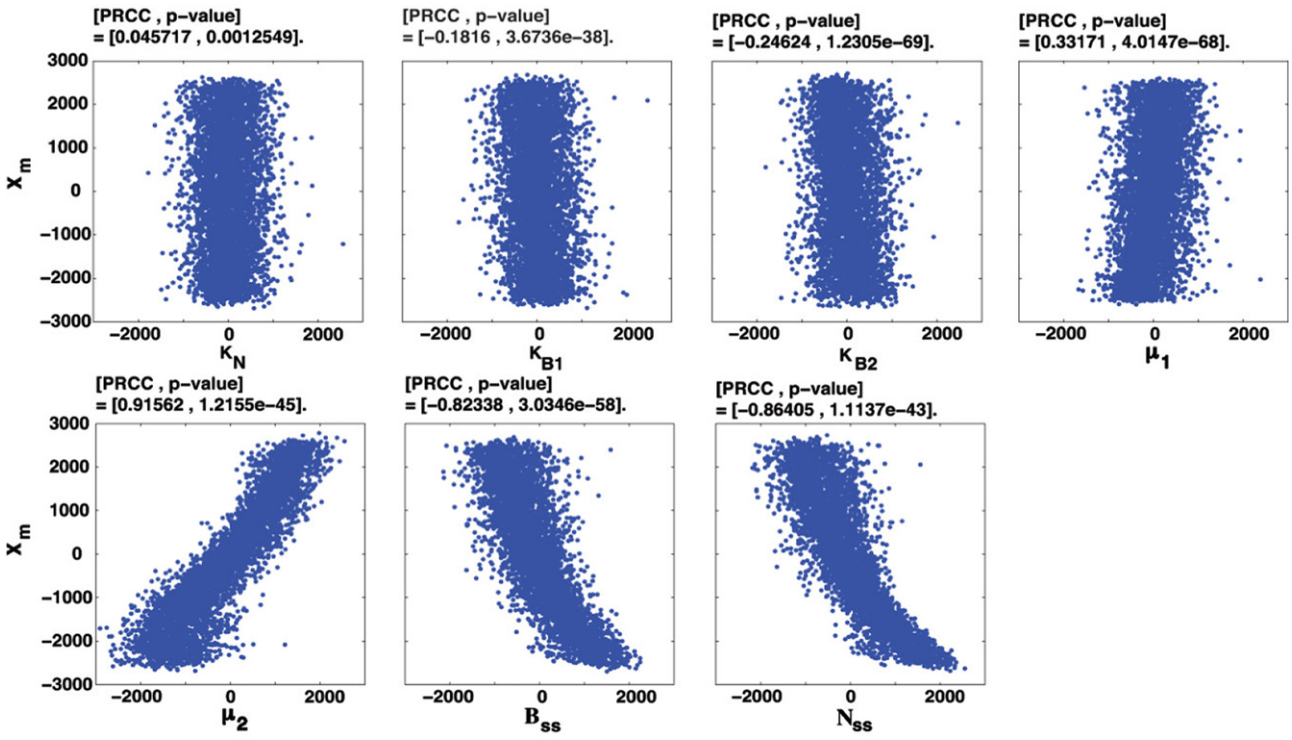

Fig. 6. Scatter plots of rank transformed x_m at 720 h versus some rank transformed parameters with statistically significant correlation (p-value < 0.01). The title of each subplot shows its PRCC value and significance.

factors", have only been roughly estimated. We performed sensitivity analysis on the normalizing factors in order to establish stability of the simulation results.

The paper should be viewed as setting up a conceptual framework for amore detailed data-based study, which should include additional signaling pathways associated with *APC* mutation and other mutations, such as *RAS* and *RAF*, which often occur in colon cancer progression and metastasis.

Acknowledgments

This research has been supported by the Mathematical Biosciences Institute and the National Science Foundation under Grant DMS 0931642.

Appendix A. Parameters estimation

A.1. Mucins

$\boldsymbol{\lambda_{12}}$: The half life of MUC1 is around 16.5 h (Pimental et al., 1996); thus we take a degradation rate of MUC1 of $\lambda_{12} = (\ln(2)/16.5)\ \mathrm{h}^{-1} = 1.17\times10^{-5}\ \mathrm{s}^{-1}$ in Eq. (11).

$\boldsymbol{\lambda_{11}}, \boldsymbol{K_1}, \boldsymbol{\alpha}$: To estimate λ_{11} and K_1, we shall use the steady state values of MUC1 (M_{1ss}) and NF-κB (N_{ss}) for healthy colon and for tumor colon. For healthy tissue, $M_{1ss} = 0.5\text{–}2\ \mu\mathrm{g/cm^3}$ (Agrawal et al., 1998); we take $M_{1ss} = 1.25\times10^{-6}\ \mathrm{g/cm^3}$. Next, according to Hoffmann et al. (2002), the steady state concentration of NF-κB for healthy tissue is around 0.04 μM where 1 M = 1 Molar = 1 mol/L = 1 mol/dm^3, 1 mol is the amount of a substance that contains as many entities as there are atoms in 12 g of ^{12}C. Since the weight of NF-κB molecule is 60 kDa where 1 Da = 1 g/mol (1 Da is 1/12 of the rest mass of ^{12}C), we get $N_{ss} = (0.04\times60)(\mu\mathrm{M}\times\mathrm{kDa}) = 2.4\times(10^{-9}\times10^{3})\ \mathrm{g/cm^3} = 2.4\times10^{-6}\ \mathrm{g/cm^3}$. In colon tumor, the concentration of MUC1 is 50% more than that of healthy tissue (Saeland et al., 2012) while the concentration of NF-κB is double that of healthy tissue (Kojima et al., 2004). Hence we get two steady state equations for solving α, λ_{11} and K_1

$$\lambda_{11}+\alpha\frac{N_{ss}}{N_{ss}+K_1}-\lambda_{12}M_{1ss}=0, \tag{A.1}$$

$$\lambda_{11}+\alpha\frac{2N_{ss}}{2N_{ss}+K_1}-\lambda_{12}(1.5M_{1ss})=0. \tag{A.2}$$

We shall take K_1 to be at least 10 times larger than N_{ss}. The effect of NF-κB on MUC1 production should be at least comparable to the production when there is no infection. Hence, the term $\alpha N_{ss}/(N_{ss}+K_1)$ should not be too small compared to λ_{11}; we take it to be $\alpha = 20\lambda_{11}$. Then, from Eqs. (A.1) and (A.2), we obtain $K_1 = 3.36\times10^{-5}\ \mathrm{g/cm^3}$, $\lambda_{11} = 6.26\times10^{-12}\ \mathrm{gs^{-1}/cm^3}$ and $\alpha = 20$ $\lambda_{11} = 1.25\times10^{-10}\ \mathrm{g/(cm^3\ s)}$.

$\boldsymbol{\lambda_{22}}$: Estimates of the MUC2 turnover in the distal colon suggest a half-life of a few hours (Hansson, 2011); thus we assume that half life of MUC2 is around 3 h and the degradation rate coefficient of MUC2 in Eq. (12) is then $(\ln(2)/3)\ \mathrm{h}^{-1} = 2.79\times10^{-5}\ \mathrm{s}^{-1}$.

$\boldsymbol{D_M}$: The diffusion rate D_M of MUC2 in mucus layer is similar to that of human cervical mucin in water (Axelsson et al., 1998), which is $4.7\times10^{-8}\ \mathrm{cm^2/s}$ (Sheehan and Carlstedt, 1984).

$\boldsymbol{K_2}$, $\boldsymbol{\beta}$, $\boldsymbol{\lambda_{21}}$: For healthy colon, the density of MUC2 is around $M_{2ss} = 1.3\ \mathrm{g/cm^3}$ (Aksoy et al., 1999) and the thickness of mucus layer is around $x_{top} = 0.01$ cm (Atuma et al., 2001; Corfield et al., 2001), so the steady state, $\hat{M}_{2ss}$, of total amount of MUC2 is $\int_0^{x_{top}} M_{2ss}\,dx = M_{2ss}\times x_{top} = 1.3\times10^{-2}\ \mathrm{g/cm^2}$. From the steady state equation of (12), we get

$$\lambda_{21}(p)+\beta\frac{N_{ss}}{N_{ss}+K_2}=\frac{\lambda_{22}\hat{M}_{2ss}}{D_M}. \tag{A.3}$$

We assume that the relative change of MUC2 in tumor colon is comparable to the increase in MUC1 concentration, so we take $\beta = 20\lambda_{21}(p)$ and $K_2 = K_1 = 3.36\times10^{-5}\ \mathrm{g/cm^3}$ in Eq. (12). From Eq. (A.3), we then obtain $\lambda_{21}(p) = 3.31\ \mathrm{g/cm^4}$ for healthy tissue, and then $\beta = 20\lambda_{21}(p) = 66.15\ \mathrm{g/cm^4}$.

A.2. Chronic inflammation

μ_1 and μ_2 are normalizing factors of M_1 and $\hat{M}_2$, respectively. We assume that MUC2 blocks inflammation better than MUC1 and take $\mu_1 = 10M_{1ss} = 1.25\times10^{-5}\ \mathrm{g/cm^3}$ and $\mu_2 = \hat{M}_{2ss} = 1.3\times10^{-2}\ \mathrm{g/cm^2}$.

A.3. NF-κB

$\boldsymbol{\lambda_{31}}$, $\boldsymbol{\lambda_{32}}$: As mentioned before, the steady state N_{ss} of NF-κB in healthy tissue is $N_{ss} = 2.4\times10^{-6}\ \mathrm{g/cm^3}$ (Hoffmann et al., 2002). This number equals to $\lambda_{31}/\lambda_{32}$ when $I=0$ (no inflammation) in Eq. (13). On the other hand, the deactivation rate λ_{32} of NF-κB is estimated by nuclear export rate (into the nuclear) of NF-κB which is equal to $\lambda_{32} = 8\times10^{-5}\ \mathrm{s^{-1}}$ (Hoffmann et al., 2002). Hence $\lambda_{31} = N_{ss}\lambda_{32} = (2.4\times10^{-6}\ \mathrm{g/cm^3})\times\lambda_{32} = 1.92\times10^{-10}\ \mathrm{g/(cm^3\ s)}$.

$\boldsymbol{K_N}$: Note, by (13), that I decreases when M_1 and $\hat{M}_2$ increase, and K_N is the normalizing factor of I. The range of I is from 0 to 1, and we shall take $K_N = 0.1$.

$\boldsymbol{\gamma}$: From Eq. (13), the steady state concentration of NF-κB for tumor colon (I/K_N is large) is $(1+\gamma)\lambda_{31}/\lambda_{32}$, whereas in healthy tissue it is $\lambda_{31}/\lambda_{32}$. Since the concentration of NF-κB in tumor colon is double that of health tissue (Kojima et al., 2004), we get $\gamma = 1$.

A.4. β-catenin

$\boldsymbol{\lambda_{41}}$, $\boldsymbol{\lambda_{42}}$: In Murray et al. (2010), the production rate λ_{41} and the degradation coefficient λ_{42} of β-catenin in a natural-turnover (destruction-complex-independent manner) are $\lambda_{41} = 25.38\ \mathrm{nM/h}$ and $\lambda_{42} = 1.54\times10^{-2}\ \mathrm{h^{-1}} = 4.28\times10^{-6}\ \mathrm{s^{-1}}$, respectively. Since the weight of β-catenin is around 92 kDa, we get $\lambda_{41} = 92\times25.38\times10^{-12}\ \mathrm{kg/(cm^3\ h)} = 6.49\times10^{-10}\ \mathrm{gs^{-1}/cm^3}$ in Eq. (14).

$\boldsymbol{K_{B1}}$,$\boldsymbol{K_{B2}}$: In Eq. (14), K_{B1} is the normalizing factor of M_1, so we take it to be $K_{B1} = M_{1ss} = 1.25\times10^{-6}\ \mathrm{g/cm^3}$. Similarly, we take $K_{B2} = K_N = 0.1$.

$\boldsymbol{\nu_1}$, $\boldsymbol{\nu_2}$: *APC* mutation cells exhibit over 8-fold increased concentration of β-catenin (Aust et al., 2001; Murray et al., 2010). According to Eq. (14), ν_2 should be larger than 7; we take $\nu_2 = 8$. In the abnormal tissue with no *APC* mutation, the fold change of β-catenin level is appreciably less than that in the tissue with *APC* mutation (Aust et al., 2001; Ninomiya et al., 2000); correspondingly we take $\nu_1 = \frac{1}{2}\nu_2 = 4$.

A.5. Tumor cell

According to Eq. (14), for healthy tissue ($I=0$), $B_{ss} = (\lambda_{41}/\lambda_{42})(1+\nu_2+\nu_1/(1+(M_{1ss}/K_{B1})))^{-1} = 1.37\times10^{-5}\ \mathrm{g/cm^3}$. In Eq. (17), we take $N_{ss} = 2.4\times10^{-6}\ \mathrm{g/cm^3}$.

For healthy colon, the proliferation rate λ_C should be zero. In Eq. (17), λ_C equals $\lambda_{51}(1.8-K_C)^+/(1.8-K_C)^+ + 1$ for healthy colon, so K_C has to be larger than 1.8; thus we take $K_C = 1.9$. It is difficult

Table B1
Parameters used in Eqs. (11) and (12).

Parameter	Value	Definition	References
MUC1			
M_{1ss}	1.25×10^{-6} g/cm^3	Steady state concentration of MUC1 for healthy tissue	Agrawal et al. (1998)
λ_{11}	6.26×10^{-12} gs^{-1}/cm^3	Production parameter of MUC1	Estimated from Agrawal et al. (1998), Saeland et al. (2012), Hoffmann et al. (2002), Kojima et al. (2004)
λ_{12}	1.17×10^{-5} s^{-1}	Degradation parameter of MUC1	Pimental et al. (1996)
α ($=20\lambda_{11}$)	1.25×10^{-10} gs^{-1}/cm^3	Upregulation rate parameter of MUC1 by NF-κB	Estimated from Agrawal et al. (1998), Saeland et al. (2012), Hoffmann et al. (2002), Kojima et al. (2004)
K_1	3.36×10^{-5} g/cm^3	Upregulation parameter of MUC1 by NF-κB	Estimated from Agrawal et al. (1998), Saeland et al. (2012), Hoffmann et al. (2002), Kojima et al. (2004)
MUC2			
$\hat{M}_{2ss}$	1.3×10^{-2} g/cm^2	Steady state concentration of total MUC2 for healthy tissue	Estimated from Aksoy et al. (1999), Atuma et al. (2001), Corfield et al. (2001)
D_M	4.7×10^{-8} cm^2 s^{-1}	Diffusion coefficient of MUC2	Axelsson et al. (1998)
$\lambda_{21}(p)$	0–3.31 g/cm^4	Production parameter of MUC2 (without mutation)	Variable
λ_{22}	2.79×10^{-5} s^{-1}	Degradation parameter of MUC2	Estimated from Hansson (2011)
β	66.15 g/cm^4	Upregulation rate parameter of MUC2 by NF-κB	This work
K_2 ($=K_1$)	3.36×10^{-5} g/cm^3	Upregulation parameter of MUC2 by NF-κB	This work

Table B2
Parameters used in Eqs. (13)–(17).

Parameter	Value	Definition	References
NF-κB			
N_{ss}	2.4×10^{-6} g/cm^3	Steady state concentration of NF-κB for healthy tissue	Hoffmann et al. (2002)
λ_{31}	1.92×10^{-10} gs^{-1}/cm^3	Activation parameter of NF-κB	Estimated by Hoffmann et al. (2002)
λ_{32}	8×10^{-5} s^{-1}	Deactivation parameter of NF-κB	Hoffmann et al. (2002)
γ	1	Upregulation parameter of NF-κB by inflammation	Estimated from Kojima et al. (2004)
K_N	0.1	Normalizing factor of I	This work
β-catenin			
λ_{41}	6.49×10^{-10} gs^{-1}/cm^3	Production rate of β-catenin	Murray et al. (2010)
λ_{42}	4.28×10^{-6} s^{-1}	Degradation parameter of β-catenin	Murray et al. (2010)
ν_1	4	Upregulation parameter of β-catenin by MUC1	Estimated from Aust et al. (2001), Ninomiya et al. (2000)
ν_2	8	Upregulation parameter of β-catenin by *APC* mutation induced by inflammation	Estimated from Aust et al. (2001), Murray et al. (2010)
K_{B1}	1.25×10^{-6} g/cm^3	Normalizing factor of M_1	This work
K_{B2}	0.1	Normalizing factor of I	This work
B_{ss}	1.37×10^{-5} g/cm^3	Steady state concentration of β-catenin for healthy tissue	This work
η_A	0–2	Parameter controlling the level of *APC* mutation	Variable
Inflammation			
μ_1	1.25×10^{-5} g/cm^3	Normalizing factor of M_1	This work
μ_2	1.3×10^{-2} g/cm^2	Normalizing factor of $\hat{M}_2$	This work
Tumor cell			
λ_{51}	1.5×10^{-6} s^{-1}	Proliferation parameter of tumor cell	Eisenberg et al. (2011), Kim and Friedman (2010), Kim et al. (2010)
K_C	1.9	Threshold of normalized B and N	This work

Table B3
PRCC values and ranges of parameters for the PRCC simulations.

Parameter	Range	PRCC
λ_{11}	$[3.13,9.39]10^{-12}$ gs^{-1}/cm^3	0.0005
λ_{12}	$[0.585,1.755]10^{-5}$ s^{-1}	0.0341
α	$[0.625,1.875]10^{-10}$ gs^{-1}/cm^3	0.0315
K_1	$[1.68,5.04]10^{-5}$ g/cm^3	−0.0064
D_M	$[2.35,7.05]10^{-8}$ cm^2 s^{-1}	0.0090
λ_{22}	$[1.395,4.185]10^{-5}$ s^{-1}	0.0023
β	[33.075,99.225] g/cm^4	−0.0068
K_2	$[1.68,5.04]10^{-5}$ g/cm^3	0.0120
λ_{31}	$[0.96,2.88]10^{-10}$ gs^{-1}/cm^3	−0.0037

Table B3 (*continued*)

Parameter	Range	PRCC
λ_{32}	$[4,12]10^{-5}$ s^{-1}	−0.0075
γ	[0.5,1.5]	−0.0101
K_N	[0.05,0.15]	0.0457[a]
λ_{41}	$[3.245,9.735]10^{-10}$ gs^{-1}/cm^3	0.0189
λ_{42}	$[2.14,6.42]10^{-6}$ s^{-1}	−0.0158
ν_1	[2,6]	−0.0275
ν_2	[4,12]	0.0506
K_{B1}	$[0.625,1.875]10^{-6}$ g/cm^3	−0.1816[a]
K_{B2}	[0.05,0.15]	−0.2462[a]
μ_1	$[0.625,1.875]10^{-5}$ g/cm^3	0.3317[a]
μ_2	$[0.65,1.95]10^{-2}$ g/cm^2	0.9156[a]
λ_{51}	$[0.75,2.25]10^{-6}$ s^{-1}	0.0097
B_{ss}	$[0.685,2.055]10^{-5}$ g/cm^3	−0.8234[a]
N_{ss}	$[1.2,3.6]10^{-6}$ g/cm^3	−0.8640[a]
K_C	[1,3]	0.0134

[a] Denotes significant PRCC values (p-value < 0.01).

to determine directly the proliferation rate of colon cancer, but in other cancers, rates of order 10^{-6} s^{-1} were used (Eisenberg et al., 2011; Kim and Friedman, 2010; Kim et al., 2010). We correspondingly take $\lambda_{51} = 1.5 \times 10^{-6}$ s^{-1}.

Appendix B. Tables

(See Tables B1–B3).

References

Aggarwal, B.B., Shishodia, S., Sandur, S.K., Pandey, M.K., Sethi, G., 2006. Inflammation and cancer: how hot is the link? Biochem. Pharmacol. 72 (11), 1605–1621.

Agrawal, B., Krantz, M.J., Reddish, M.A., Longenecker, B.M., 1998. Cancer-associated MUC1 mucin inhibits human T-cell proliferation, which is reversible by IL-2. Nat. Med. 4, 43–49.

Aksoy, N., Thornton, D.J., Corfield, A., Paraskeva, C., Sheehan, J.K., 1999. A study of the intracellular and secreted forms of the MUC2 mucin from the PC/AA intestinal cell line. Glycobiology 9 (7), 739–746.

Allen, A., Hutton, D.A., Pearson, J.P., 1998. The MUC2 gene product: a human intestinal mucin. Int. J. Biochem. Cell Biol. 30, 797–801.

Atuma, C., Strugala, V., Allen, A., Holm, L., 2001. The adherent gastrointestinal mucus gel layer: thickness and physical state in vivo. Am. J. Physiol. Gastrointest. Liver Physiol. 280 (5), G922–G929.

Aust, D.E., Terdiman, J.P., Willenbucher, R.F., Chew, K., Ferrell, L., Florendo, C., Molinaro-Clark, A., Baretton, G.B., Lohrs, U., Waldman, F.M., 2001. Altered distribution of beta-catenin, and its binding proteins E-cadherin and APC, in ulcerative colitis-related colorectal cancers. Mod. Pathol. 14 (1), 29–39.

Axelsson, M.A.B., Asker, N., Hansson, G.C., 1998. O-glycosylated MUC2 monomer and dimer from ls 174t cells are water-soluble, whereas larger MUC2 species formed early during biosynthesis are insoluble and contain nonreducible intermolecular bonds. J. Biol. Chem. 273 (30), 18864–18870.

Bienz, M., Hamada, F., 2004. Adenomatous polyposis coli proteins and cell adhesion. Curr. Opin. Cell Biol. 16 (5), 528–535.

Byrd, J.C., Bresalier, R.S., 2004. Mucins and mucin binding proteins in colorectal cancer. Cancer Metastasis Rev. 23, 77–99.

Calvisi, D.F., Ladu, S., Factor, V.M., Thorgeirsson, S.S., 2004. Activation of beta-catenin provides proliferative and invasive advantages in c-myc/TGF-alpha hepatocarcinogenesis promoted by phenobarbital. Carcinogenesis 25 (6), 901–908.

Chen, S., Liu, J., Li, G., Mo, F., Xu, X., Zhang, T., Zhang, X., Li, J., Han, X., Sun, Y., 2008. Altered distribution of beta-catenin and prognostic roles in colorectal carcinogenesis. Scand. J. Gastroenterol. 43 (4), 456–464.

Corfield, A.P., Carroll, D., Myerscough, N., Probert, C.S., 2001. Mucins in the gastrointestinal tract in health and disease. Front Biosci. 6, D1321–D1357.

Delitala, M., Lorenzi, T., 2011. A mathematical model for progression and heterogeneity in colorectal cancer dynamics. Theor. Popul. Biol. 79, 130–138.

Eisenberg, M.C., Kim, Y., Li, R., Ackerman, W.E., Kniss, D.A., Friedman, A., 2011. Mechanistic modeling of the effects of myoferlin on tumor cell invasion. Proc. Natl. Acad. Sci. USA 108, 20078–20083.

Femia, A.P., Dolara, P., Giannini, A., Salvadori, M., Biggeri, A., Caderni, G., 2007. Frequent mutation of Apc gene in rat colon tumors and mucin-depleted foci, preneoplastic lesions in experimental colon carcinogenesis. Cancer Res. 67 (2), 445–449.

Ferlay, J., Shin, H.R., Bray, F., Forman, D., Mathers, C., Parkin, D.M., 2010. Estimates of worldwide burden of cancer in 2008: GLOBOCAN 2008. Int. J. Cancer 127, 2893–2917.

Hansson, G., 2011. Role of mucus layers in gut infection and inflammation. Curr. Opin. Microbiol. 15, 57–62.

Hoffmann, A., Levchenko, A., Scott, M.L., Baltimore, D., 2002. The IkappaB-NF-kappaB signaling module: temporal control and selective gene activation. Science 298 (5596), 1241–1245.

Huang, L., Ren, J., Chen, D., Li, Y., Kharbanda, S., Kufe, D., 2003. MUC1 cytoplasmic domain coactivates Wnt target gene transcription and confers transformation. Cancer Biol. Ther. 2 (6), 702–706.

Humphries, A., Wright, N.A., 2008. Colonic crypt organization and tumorigenesis. Nat. Rev. Cancer 8, 415–424.

Iwashita, J., Sato, Y., Sugaya, H., Takahashi, N., Sasaki, H., Abe, T., 2003. mRNA of MUC2 is stimulated by IL-4, IL-13 or TNF-alpha through a mitogen-activated protein kinase pathway in human colon cancer cells. Immunol. Cell Biol. 81 (4), 275–282.

Johnston, M.D., Edwards, C.M., Bodmer, W.F., Maini, P.K., Chapman, S.J., 2007. Mathematical modeling of cell population dynamics in the colonic crypt and in colorectal cancer. Proc. Natl. Acad. Sci. USA 104, 4008–4013.

Karin, M., Greten, F.R., 2005. NF-kappaB: linking inflammation and immunity to cancer development and progression. Nat. Rev. Immunol. 5 (10), 749–759.

Kim, Y., Friedman, A., 2010. Interaction of tumor with its micro-environment: a mathematical model. Bull. Math. Biol. 72 (5), 1029–1068.

Kim, Y., Wallace, J., Li, F., Ostrowski, M., Friedman, A., 2010. Transformed epithelial cells and fibroblasts/myofibroblasts interaction in breast tumor: a mathematical model and experiments. J. Math. Biol. 61 (3), 401–421.

Kojima, M., Morisaki, T., Sasaki, N., Nakano, K., Mibu, R., Tanaka, M., Katano, M., 2004. Increased nuclear factor-kB activation in human colorectal carcinoma and its correlation with tumor progression. Anticancer Res. 24 (2B), 675–681.

Kufe, D.W., 2009. Functional targeting of the MUC1 oncogene in human cancers. Cancer Biol. Ther. 8 (13), 1197–1203.

Kwong, L.N., Dove, W.F., 2009. Apc and its modifiers in colon cancer. Adv. Exp. Med. Biol. 656, 85–106.

Li, J.D., Feng, W., Gallup, M., Kim, J.H., Gum, J., Kim, Y., Basbaum, C., 1998. Activation of NF-kappaB via a Src-dependent Ras-MAPK-pp90rsk pathway is required for *Pseudomonas aeruginosa*-induced mucin overproduction in epithelial cells. Proc. Natl. Acad. Sci. USA 95 (10), 5718–5723.

Linden, S.K., Florin, T.H.J., McGuckin, M.A., 2008. Mucin dynamics in intestinal bacterial infection. PLoS One 3 (12), e3952.

Marino, S., Hogue, I.B., Ray, C.J., Kirschner, D.E., 2008. A methodology for performing global uncertainty and sensitivity analysis in systems biology. J. Theor. Biol. 254, 178–196.

McGuckin, M.A., Linden, S.K., Sutton, P., Florin, T.H., 2011. Mucin dynamics and enteric pathogens. Nat. Rev. Microbiol. 9 (4), 265–278.

Michor, F., Iwasa, Y., Lengauer, C., Nowak, M.A., 2005. Dynamics of colorectal cancer. Semin. Cancer Biol. 15, 484–493.

Murray, P.J., Kang, J.-W., Mirams, G.R., Shin, S.-Y., Byrne, H.M., Maini, P.K., Cho, K.-H., 2010. Modelling spatially regulated beta-catenin dynamics and invasion in intestinal crypts. Biophys. J. 99, 716–725.

Ninomiya, I., Endo, Y., Fushida, S., Sasagawa, T., Miyashita, T., Fujimura, T., Nishimura, G., Tani, T., Hashimoto, T., Yagi, M., Shimizu, K., Ohta, T., Yonemura, Y., Inoue, M., Sasaki, T., Miwa, K., 2000. Alteration of beta-catenin expression in esophageal squamous-cell carcinoma. Int. J. Cancer 84 (3), 251–257.

Ookawa, K., Kudo, T., Aizawa, S., Saito, H., Tsuchida, S., 2002. Transcriptional activation of the MUC2 gene by p53. J. Biol. Chem. 277 (50), 48270–48275.

Pimental, R.A., Julian, J., Gendler, S.J., Carson, D.D., 1996. Synthesis and intracellular trafficking of MUC-1 and mucins by polarized mouse uterine epithelial cells. J. Biol. Chem. 271 (45), 28128–28137.

Rowan, A.J., Lamlum, H., Ilyas, M., Wheeler, J., Straub, J., Papadopoulou, A., Bicknell, D., Bodmer, W.F., Tomlinson, I.P.M., 2000. Apc mutations in sporadic colorectal tumors: a mutational "hotspot" and interdependence of the "two hits". Proc. Natl. Acad. Sci. USA 97 (7), 3352–3357.

Saeland, E., Belo, A., Mongera, S., van Die, I., Meijer, G., van Kooyk, Y., 2012. Differential glycosylation of MUC1 and CEACAM5 between normal mucosa and tumour tissue of colon cancer patients. Int. J. Cancer 131 (1), 117–128.

Sheehan, J.K., Carlstedt, I., 1984. Hydrodynamic properties of human cervical-mucus glycoproteins in 6 m-guanidinium chloride. Biochem. J. 217, 93–101.

Ueno, K., Koga, T., Kato, K., Golenbock, D.T., Gendler, S.J., Kai, H., Kim, K.C., 2008. MUC1 mucin is a negative regulator of toll-like receptor signaling. Am. J. Respir. Cell Mol. Biol. 38 (3), 263–268.

Ullman, T.A., Itzkowitz, S.H., 2011. Intestinal inflammation and cancer. Gastroenterology 140 (6), 1807–1816.

van Leeuwen, I.M.M., Byrne, H.M., Jensen, O.E., King, J.R., 2006. Crypt dynamics and colorectal cancer: advances in mathematical modelling. Cell Proliferation 39, 157–181.

van Leeuwen, I.M.M., Edwards, C.M., Ilyas, M., Byrne, H.M., 2007. Towards a multiscale model of colorectal cancer. World J. Gastroenterol. 13, 1399–1407.

Velcich, A., Yang, W., Heyer, J., Fragale, A., Nicholas, C., Viani, S., Kucherlapati, R., Lipkin, M., Yang, K., Augenlicht, L., 2002. Colorectal cancer in mice genetically deficient in the mucin Muc2. Science 295 (5560), 1726–1729.

Yamamoto, M., Bharti, A., Li, Y., Kufe, D., 1997. Interaction of the DF3/MUC1 breast carcinoma-associated antigen and beta-catenin in cell adhesion. J. Biol. Chem. 272 (19), 12492–12494.

Yang, K., Popova, N.V., Yang, W.C., Lozonschi, I., Tadesse, S., Kent, S., Bancroft, L., Matise, I., Cormier, R.T., Scherer, S.J., Edelmann, W., Lipkin, M., Augenlicht, L., Velcich, A., 2008. Interaction of MUC2 and Apc on Wnt signaling and in intestinal tumorigenesis: potential role of chronic inflammation. Cancer Res. 68 (18), 7313–7322.